第 31 卷第 7 期
2015 年 7 月

无 机 化 学 学 报
CHINESE JOURNAL OF INORGANIC CHEMISTRY

Vol.31 No.7
1460-1466

氰根桥连的 $Fe^{Ⅲ}Mn^{Ⅱ}$ 链中磁性作用的调控

郑 慧 徐 杨 段春迎*

(大连理工大学精细化工重点实验室,大连 116024)

摘要: 基于三氰构筑单元合成了两个氰基桥联的 $Fe^{Ⅲ}$-$Mn^{Ⅱ}$ 一维链,{[Fe(Tp)$(CN)_3]_2$[Mn(bib)]}·CH_3OH·$2H_2O$ (**1**)和{[Fe(pzTp)$(CN)_3]_2$[Mn(bib)]}·$3H_2O$ (**2**)。**1** 和 **2** 中的双之字链通过刚性的双齿配体固定排列方式并连接成二维结构,链内 $Fe^{Ⅲ}$和 $Mn^{Ⅱ}$之间的磁相互作用可以通过改变链中配体的位阻调控。

关键词: 氰基; 之字链; 双齿配体; 磁相互作用
中图分类号: 0614.7 **文献标识码**: A **文章编号**: 1001-4861(2015)07-1460-07
DOI:10.11862/CJIC.2015.177

Tuning Intrachain Magnetic Interactions of Cyanide-bridged $Fe^{Ⅲ}Mn^{Ⅱ}$ Chain

ZHENG Hui XU Yang DUAN Chun-Ying*

(*State Key Laboratory of Fine Chemicals, Dalian University of Technology, Dalian*, 116024, *China*)

Abstract: Two cyanide bridged $Fe^{Ⅲ}$-$Mn^{Ⅱ}$ double zigzag chains {[Fe(Tp)$(CN)_3]_2$[Mn(bib)]}·CH_3OH·$2H_2O$ (**1**) and {[Fe(pzTp)$(CN)_3]_2$[Mn(bib)]}·$3H_2O$ (**2**) were synthesized utilizing tricyanometallate building blocks. The chains were further linked via long ditopic ligand to form two dimensional compounds. With the alignment of chains fixed by the rigid ditopic linker, the intrachain magnetic interactions between $Fe^{Ⅲ}$ and $Mn^{Ⅱ}$ could be further tuned via changing the capping ligand of $Fe^{Ⅲ}$ ions. CCDC: 1001946, **1** ; 1001947, **2**.

Key words: cyanide; zigzag chain; ditopic linker; magnetic interactions

0 Introduction

One-dimensional magnetic systems, especially single chain magnets (SCMs), are attracting considerable interest in the field of chemistry, physics and material science[1]. Such materials present both spontaneous magnetization and quantum behavior, providing an ideal model for studying the coexistence of classic and quantum behavior[2-5]. Moreover, SCMs can retain spin information over long periods of time, providing potential applications in high-density information storage, quantum computing, and spintronics[6-7]. Thereinto, cyanide-bridged complexes are of particular interest, because their structures can be rationally designed utilizing the linear linking mode of cyano-bridge of cyanometallate[8-10]. Moreover, it is possible to reasonably predict the type of magnetic interaction and in some cases the magnitude of the magnetic anisotropy with knowledge of the exchange interaction nature through the cyanide bridge[11-12]. In these systems, metal ions with strong anisotropy are usually adopted. However, the apical directions of the metal ions are not uniform and are tilted with an angle in general case, which will decrease the blocking temperature of the system or destroy the SCMs behavior[13]. Even if the apical directions of

收稿日期:2015-04-07。收修改稿日期:2015-05-08。
国家自然科学基金(No.91122031)资助项目。
*通讯联系人。E-mail:cyduan@dlut.edu.cn;会员登记号:S06N6732S1406。

metal ions within one chain are parallel, the apical directions of metal ions in neighboring chains may be different. In this case, the anisotropy of the system is hard to increase because the neighboring chains rotate an angle relatively[14-15]. To solve this problem, a rational way is to use structurally ditopic, magnetically inert rigid organic linkers, which will link the chain into two-dimensional networks without significant changing the nature of the chains. This rigid linker can control the arrangement of chains, and force the apical directions of metal ions to parallel with each other, maximizing the anisotropy of the whole system. In the same time, the interchain interactions could also be controlled via choosing ditopic linkers with different lengths and electric natures. With such strategy, we have synthesized light-responsive SCMs, whose magnetic properties can be tuned via light-induced charge transfer or spin-crossover[16]. Both $Mn^{Ⅱ}$ ions and $Fe^{Ⅲ}$ ions possess different redox valence states, and charge transfer properties between them have been reported[17]. We aimed to incorporating $Mn^{Ⅱ}$ ions and paramagnetic $Fe^{Ⅲ}$ ions into a cyanide-bridged $\{Fe^{Ⅲ}_2Mn^{Ⅱ}\}$ chain utilizing tricyanometallate building block. Moreover, a rigid ditopic linker was adopted to fix the orientation of the chains and link the chains to form a layer. With such strategy, two heterometallic Fe-Mn compounds, $\{[Fe(Tp)(CN)_3]_2[Mn(bib)]\}\cdot CH_3OH\cdot 2H_2O$ (**1**) (Tp =hydrotris (pyrazolyl)borate; bib =1,4-bis (1-imidazolyl)benzene) and $\{[Fe(pzTp)(CN)_3]_2[Mn(bib)]\}\cdot 3H_2O$ (**2**) (pzTp=tetrakis(pyrazolyl)borate), were synthesized. Unfortunately, no charge transfer was observed. However, the interchain linkage and apical directions of $Mn^{Ⅱ}$ ions were fixed with the rigid linker, providing a chance to tune the intrachain magnetic interactions via changing the capping ligand of $Fe^{Ⅲ}$ ions of cyanometallate building blocks.

1 Experimental

1.1 Materials and physical measurements

Manganese(Ⅱ) perchloratehexahydrate ($Mn(ClO_4)_2\cdot 6H_2O$, 99%) and methanol (CH_3OH) were of analytical grade from Tianjin Kemiou Chemical Reagent Co., Ltd. China. All chemical reagents were obtained from commercial sources and were used as received without further purication unless otherwise noted. The compounds $Bu_4N[Fe(Tp)(CN)_3]$[18], $Bu_4N[Fe(pzTp)(CN)_3]$[19] and ligand bib were synthesized by a modified literature method[20]. Elemental analyses (carbon, hydrogen, and nitrogen) were carried out on an Elementar Vario EL Ⅲ analyzer. Infrared spectra were recorded as fine powder samples with a JASCO FT/IR-600 Plus spectrometer in the 400~4 000 cm^{-1} region and a spectral resolution of 1 cm^{-1}. Magnetic measurements of the samples were performed on a Quantum Design SQUID (MPMS XL-7) magnetometer. Data were corrected for the diamagnetic contribution calculated from Pascal constants.

1.2 Preparation of complexes 1 and 2

1.2.1 Synthesis of $\{[Fe(Tp)(CN)_3]_2[Mn(bib)]\}\cdot CH_3OH\cdot 2H_2O$ (**1**)

4.0 mL water solution of 0.05 mmol (18.1 mg) $Mn(ClO_4)_2\cdot 6H_2O$ was placed at the bottom in one side of an H-shaped tube, while 4.0 mL methanol solution of 0.1 mmol (58.9 mg) $[Bu_4N][Fe(Tp)(CN)_3]$ and 0.4 mmol (84.0 mg) bib was placed in the other side. Then 4.0 mL methanol solution was layered upon solutions of both sides to provide diffusion pathway. Crystallization took several weeks and gave crystals in a yield of 55% based on $Mn(ClO_4)_2\cdot 6H_2O$. Element analysis: Calcd. for $C_{37}H_{38}B_2Fe_2MnN_{22}O_3$ (%): C 43.26, H 3.73, N 30.01; Found(%): C 43.21, H 3.89, N 29.13. IR (solid KBr pellet, ν/cm^{-1}): 3 443 vs, 3 123 m, 2 508 w, 2 134 s, 2 123 s, 1 632 s, 1 530 s, 1 501 m, 1 408 s, 1 313 s, 1 262 w, 1 214 m, 1 116 s, 1 064 s, 1048 s, 988 w, 961 m, 929 w, 836 m, 769 m, 766 s, 711 m, 658 m, 614 m, 536 m,492 m.

1.2.2 Synthesis of $\{[Fe(pzTp)(CN)_3]_2[Mn(bib)]\}\cdot 3H_2O$ (**2**)

The preparation of complex **2** was carried out using a procedure similar to that employed for complex **1**. $[Bu_4N][Fe(pzTp)(CN)_3]$ (0.1 mmol, 65.5 mg) was used as the building block, and the red prisms crystals were obtained in a yield of 70% based on $Mn(ClO_4)_2\cdot 6H_2O$. Element analysis: Calcd. for $C_{42}H_{41}B_2Fe_2MnN_{26}O_3$ (%): C 44.01, H 3.60, N 31.77; Found(%): C 44.09, H 3.65, N 31.70. IR (solid KBr pellet, ν/cm^{-1}): 3 439 vs,

3 137 m, 2 141 m, 1 633 m, 1 530 s, 1 501 m, 1 441 w, 1 408 s, 1 388 m, 1 307 s, 1 243 w, 1 213 s, 1 107 s, 1 092 w, 1 065 s, 962 w, 932 w, 858 m, 809 m, 794 m, 768 s, 655 m, 614 m, 536 m.

1.3 Crystallographic refinement details

The data was collected on a Bruker Smart APEX Ⅱ X-diffractometer equipped with graphite monochromatic Mo $K\alpha$ radiation (λ=0.071 073 nm) using the SMART and SAINT programs. Indexing and unit cell refinement were based on all observed reflections. The structures were solved in the space group by direct method and refined by the full-matrix least-squares fitting on F^2 using SHELXTL-97. All non-hydrogen atoms were treated anisotropically. Hydrogen atoms bound to carbon were placed in calculated positions using a riding model while those attached to some water lattice solvents were located in the difference Fourier map and refined using fixed isotropic thermal parameters based on their respective parent atoms. The details of crystallographic data for compounds **1** and **2** are listed in Table 1. Selected bond distances and angles are listed in Table 2, respectively.

CCDC:1001946, **1** ; 1001947, **2**.

Table 1 Selected crystal data and structure refinement parameters of 1 and 2

	1	**2**
Formula	$C_{37}H_{38}B_2Fe_2MnN_{22}O_3$	$C_{42}H_{41}B_2Fe_2MnN_{26}O_3$
Formula weight	1 027.15	1 146.27
Crystal system	Monoclinic	Monoclinic
Space group	$P2_1/c$	$P2_1/c$
a / nm	1.414(4)	1.467(7)
b / nm	2.505(7)	2.709(15)
c / nm	1.585(6)	1.427(8)
β / (°)	118.6(2)	101.5(2)
V / nm^3	4.928(3)	5.562(5)
Z	4	4
D_c / (g·cm^{-3})	1.384	1.369
μ(Mo $K\alpha$) / mm^{-1}	0.892	0.8
F(000)	2 099	2 344
θ_{min}, θ_{max} / (°)	2.19, 25.00	1.06, 25.00
Index range	$-16 \leqslant h \leqslant 12$, $-28 \leqslant k \leqslant 29$, $-18 \leqslant l \leqslant 18$	$-12 \leqslant h \leqslant 17$, $-22 \leqslant k \leqslant 32$, $-16 \leqslant l \leqslant 16$
No. total reflns.	16 820	29 602
No. uniq. reflns (R_{int})	8 647 (0.033 5)	9 793 (0.041 6)
No. obs. [$I \geqslant 2\sigma(I)$]	8 647	9 793
No. params	613	685
R_1, wR_2 [$I \geqslant 2\sigma(I)$]	0.079 7, 0.226 4	0.064 3, 0.203 2
R_1, wR_2 (all data)	0.099 1, 0.239 0	0.089 9, 0.218 5
GOF on F^2	1.056	1.038

$R_1=\sum(|F_o|-|F_c|)/\sum|F_o|$; $wR_2=[\sum w(|F_o|-|F_c|)^2/\sum wF_o^2]^{1/2}$.

Table 2 Selected bond distances (nm) and angles (°) in 1 and 2

1					
Fe(1)-C(10)	0.189 9(6)	Mn(1)-N(8)	0.220 2(5)	Fe(2)-C(27)	0.185 1(11)
Fe(1)-C(11)	0.189 8(6)	Mn(1)-N(7)	0.220 3(5)	Fe(2)-C(26)	0.190 4(7)
Fe(1)-C(12)	0.192 8(6)	Mn(1)-N(12)	0.221 8(5)	Fe(2)-C(25)	0.190 9(7)
Fe(1)-N(2)	0.197 5(5)	Mn(1)-N(10)	0.221 7(5)	Fe(2)-N(17)	0.196 0(7)
Fe(1)-N(6)	0.197 8(5)	Mn(1)-N(15)	0.222 4(5)	Fe(2)-N(19)	0.197 0(8)

Continued Table 1

Fe(1)-N(4)	0.198 1(5)	Mn(1)-N(14)	0.224 1(5)	Fe(2)-N(21)	0.197 5(8)
C(10)-Fe(1)-C(11)	84.0(2)	N(7)-C(10)-Fe(1)	174.5(5)	C(25)-N(14)-Mn(1)	144.0(5)
N(8)-Mn(1)-N(7)	97.70(2)	N(8)-C(11)-Fe(1)	174.8(5)	C(26)-N(15)-Mn(1)	145.9(5)
C(10)-N(7)-Mn(1)	156.4(5)	C(26)-Fe(2)-C(25)	85.50(3)	N(14)-C(25)-Fe(2)	173.5(6)
C(11)-N(8)-Mn(1)	156.0(5)	N(15)-Mn(1)-N(14)	91.30(2)	N(15)-C(26)-Fe(2)	174.8(6)
2					
Fe(1)-C(14)	0.192 2(5)	Mn(1)-N(26)	0.222 6(4)	Fe(3)-C(40)	0.191 4(7)
Fe(1)-C(15)	0.192 3(5)	Mn(1)-N(12)	0.223 9(4)	Fe(3)-C(42)	0.191 5(5)
Fe(1)-C(13)	0.192 5(6)	Mn(1)-N(25)	0.224 0(4)	Fe(3)-C(41)	0.192 6(5)
Fe(1)-N(4)	0.196 2(4)	Mn(1)-N(11)	0.224 0(4)	Fe(3)-N(20)	0.195 6(4)
Fe(1)-N(7)	0.197 0(4)	Mn(1)-N(10)	0.224 5(4)	Fe(3)-N(16)	0.197 1(4)
Fe(1)-N(6)	0.197 3(4)	Mn(1)-N(14)	0.224 8(4)	Fe(3)-N(22)	0.198 1(4)
C(14)-Fe(1)-C(15)	85.07(19)	N(10)-C(14)-Fe(1)	175.6(4)	C(41)-N(25)-Mn(1)	152.7(4)
N(11)-Mn(1)-N(10)	89.76(15)	N(11)-C(15)-Fe(1)	175.7(4)	C(42)-N(26)-Mn(1)	153.1(4)
C(14)-N(10)-Mn(1)	147.6(4)	C(42)-Fe(3)-C(41)	85.90(2)	N(25)-C(41)-Fe(3)	175.4(4)
C(15)-N(11)-Mn(1)	149.3(4)	N(26)-Mn(1)-N(25)	94.13(16)	N(26)-C(42)-Fe(3)	174.4(5)

2　Results and discussion

2.1　Crystal structure of compound 1 and 2

Single-crystal X-ray diffraction analysis revealed that compound **1** crystallizes in a monoclinic $P2_1/c$ space group. The crystal structure comprises neutral bimetallic $[Fe^{Ⅲ}(Tp)(CN)_3]_2Mn^{Ⅱ}(bib)$ layers, with uncoordinated water and methanol molecules located between the layers. In the neutral chain, the $[Fe(Tp)(CN)_3]^-$ unit bridges two $Mn^{Ⅱ}$ ions through two of its three cyanide groups in the *cis* position, whereas each $Mn^{Ⅱ}$ coordinates to four nitrogen atoms from the CN^- bridges, forming double zigzag chains (Fig.1a), which is similar to the reported examples[21-22]. The neutral chains are further linked by bib ligands along the apical directions of the manganese centers to a layer framework (Fig.1b). The crystal unit consists of two $Fe^{Ⅲ}$ centers and one unique $Mn^{Ⅱ}$ center. Each $Fe^{Ⅲ}$ center is located in an octahedral environment with three nitrogen atoms from the tridentate Tp unit and three

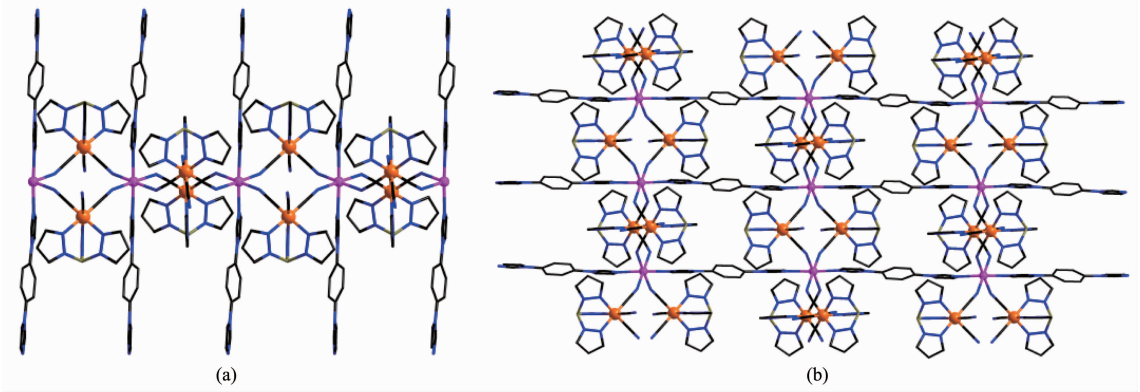

Fig.1　(a) Side view of 1D double zigzag chain of complex **1**, (b) Side view of the 2D layer for complex **1**; Hydrogen atoms and crystallization water molecules are omitted for clarity; Atoms not involved in bridging are omitted for clarity; Fe orange; Mn pink; C dark; N blue; B dark yellow

cyanide carbon atoms, whereas the coordination sites of the Mn^{II} center are occupied by two nitrogen atoms from the bidentate bib and four cyanide nitrogen atoms in an compressed N_6 coordination sphere. At 296 K, The Mn-N_{CN} bond lengths are 0.220 2~0.224 1 nm and the Mn-N_{bib} bond distances are 0.221 7~0.221 8 nm, which are in good agreement with those observed previously in related compounds containing a high spin (HS) Mn^{II} ion[13]. The Fe^{III}-C bond distances are 0.189 9~0.192 8 nm and 0.185 1~0.190 9 nm. The Fe^{III}-N bond distances are 0.197 5~0.198 1 nm and 0.196 0~0.197 5 nm, for Fe1 and Fe2, respectively, which are typical values for LS Fe^{III} ions. In neutral double zigzag chains, the square units exhibit two orientations of their mean planes ($Fe^{III}_2Mn^{II}_2$) with a 51.2° dihedral angle (here after denoted as φ). For the bond angles related to cyano bridge and metal ions, the N-C-Fe angles are 173.5°~174.8°, deviating slightly from the strict linearity. The C-N-Mn angles are 144.0°~156.0°, departing significantly from 180°. The shortest intrachain Fe-Mn, Mn-Mn, and Fe-Fe distances are 0.498 5, 0.689 9, and 0.691 6 nm, respectively, and the shortest interchain Fe-Mn, Mn-Mn, and Fe-Fe distances are 1.349, 1.390, and 1.083 nm, respectively, along the *b* axis. The shortest interchain parallel pyrazolyl-pyrazolyl separation (0.362 nm) indicates that there exist weak interchain π-π stacking interactions along the *b* axis.

The structure of complex **2** is isostructural to that of **1**. The distortion of the square units in complex **2** is slightly smaller than that in complex **1** because the steric hindrance of $[Fe(pzTp)(CN)_3]^-$ in **2** is larger than the $[Fe(Tp)(CN)_3]^-$ unit in **1**. The φ value is 47°, smaller than that in **1**. At 296 K, the lengths of the Mn-N_{CN} coordination bonds are 0.222 6~0.224 5 nm and the Mn-N_{bib} bond distances are 0.223 9 nm and 0.224 8 nm, providing an elongated N_6 coordination environment. Within the cyano bridged squares, the N≡C-Fe bond angels are 174.4° and 175.6°, being nearly linear; whereas the C≡N-Mn angles are 147.6°~153.1°, departing slightly smaller from linearity than that of **1**. The shortest intrachains of Fe-Mn, Fe-Fe, Mn-Mn are 0.507 5, 0.712 0, and 0.706 8 nm. The shortest interchain Fe-Mn, Mn-Mn, and Fe-Fe distances are 1.122, 1.350, and 1.066 nm along the *b* axis, separating by bib, respectively. There are weak interchain interactions from parallel quasi-eclipsed stacking pyrazolyl rings from adjacent chains along the *b* axis, and the shortest distance between them is 0.362 13 nm.

2.2 Magnetic properties of complexes 1 and 2

The temperature dependent magnetic susceptibilities of complexes **1** and **2** in the form of χT vs *T* plots were measured on polycrystalline samples in the range of 2~300 K under the applied magnetic field of 1 000 Oe (Fig.2). The χT values per $Fe^{III}_2Mn^{II}$ unit at room temperature are 5.24 $cm^3 \cdot mol^{-1} \cdot K$ and 5.38 $cm^3 \cdot mol^{-1} \cdot K$ for **1** and **2**, respectively. These values are a little larger than the spin-only value of 5.125 $cm^3 \cdot mol^{-1} \cdot K$ expected for the magnetically dilute system including one high-spin Mn^{II} ion (S=5/2) and two low-spin Fe^{III} ions (S=1/2), where the spin-only value is calculated by assuming $g_{Mn}=g_{Fe}=2.0$. However, this is not surprising and simply indicates that the persistence of a residual unquenched orbital contribution due to the $^2T_{2g}$ state of low-spin Fe^{III} atoms. The effective g value of Fe^{III} is often found to be different from 2.0 because of an important orbital contribution. As the temperature is lowered, the χT value gradually decreases until 25 K, where a value of 3.70 $cm^3 \cdot mol^{-1} \cdot K$ is attained. Upon further cooling, the χT value sharply decreases to 1.26 $cm^3 \cdot mol^{-1} \cdot K$ at 2 K for **1**. For **2**, the χT values decrease smoothly down to 4.33 $cm^3 \cdot$

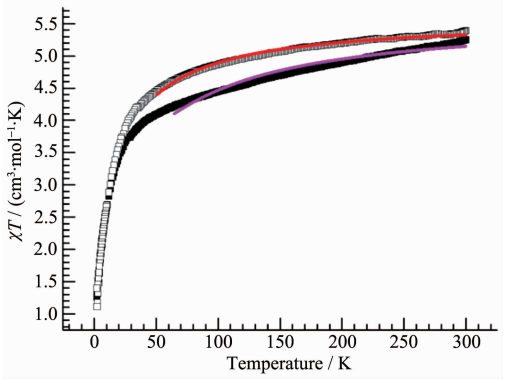

Fig.2 Temperature dependence of χT for the complexes **1** (■) and **2** (□) measured at 1 000 Oe; The solid line represents the best fit obtained with the model in Fig.3

$mol^{-1}\cdot K$ at 50 K and then abruptly reaching 1.33 $cm^3\cdot mol^{-1}\cdot K$ at 2 K. The magnetic susceptibilities data conform well to the Curie-Weiss law of 2~300 K, which gives the Curie constant of 5.35 $cm^3\cdot mol^{-1}\cdot K$ for **1** and 5.29 $cm^3\cdot mol^{-1}\cdot K$ for **2**, respectively. The negative Weiss temperatures (θ=−15.610 K for **1** and θ=−10.726 K for **2**) suggest the presence of a dominant antiferromagnetic coupling between $Fe^{Ⅲ}$ and $Mn^{Ⅱ}$ ions via the cyanide bridge within the 2D layer.

For compound **1** and **2**, to simplify the simulation model, the double zigzag chain structure could be treated as a 1D chain model (see Fig.3) and the Hamiltonian can be described as the following: $H=-2J(S_1S_2+S_1S_3+S_2S_4+S_3S_4+S_4S_5+S_4S_6+S_5S_7+S_6S_7+S_7S_8+S_7S_9+S_8S_{10}+S_9S_{10}+S_{10}S_{11}+S_{10}S_{12}+S_{11}S_1+S_{12}S_1)$, where $S_1=S_4=S_7=S_{10}=5/2$, $S_2=S_3=S_5=S_6=S_8=S_9=S_{11}=S_{12}=1/2$, and J is the coupling parameter between neighboring $Fe^{Ⅲ}$ and $Mn^{Ⅱ}$. An excellent agreement with the experimental data is obtained by calculating the susceptibility data with the MAGPACK package[21], with the following set of parameters: J=−7.64 cm^{-1}, $g=g_{Fe}=g_{Mn}$=2.09 with $R=1.99\times10^{-4}$ $\{R=\sum[(\chi_MT)_{obs}-(\chi_MT)_{cal}]^2/\sum(\chi_MT)_{obs}^2\}$ for **1**, and J=−3.78 cm^{-1}, $g=g_{Fe}=g_{Mn}$=2.04 with $R=2.16\times10^{-5}$ for **2**, respectively. As expected on the basis of their structural similarity, the magnetic behaviors of the two complexes are essentially identical. The above behaviors were consistent with an intramolecular $Fe^{Ⅲ}$-$Mn^{Ⅱ}$ antiferromagnetic interaction, which can be rationalized in terms of the magnetic orbitals of the low-spin $Fe^{Ⅲ}$ and high-spin $Mn^{Ⅱ}$ centers. An arrangement that normally gives rise to antiferromagnetic coupling. However, because of the enhancement of the steric effect of the tridentate ligand in $[LM(CN)_3]^-$ building blocks, the coupling constant J in compound **1** is over twice as large as in **2**. Therefore, the tridentate ligand in $[LM(CN)_3]^-$ building blocks plays a role in constructing molecule magnets, which not only greatly affects the structure of the resulting magnetic assemblies, but also induces a diverse hindrance effecting the different magnetic interactions. Because the steric hindrance of pzTp in **2** is larger than Tp in **1**, the bond lengths of Mn-N_{CN} in **2** are larger than that in **1**. Such difference results in that the antiferromagnetic interaction between $Fe^{Ⅲ}$-$Mn^{Ⅱ}$ ions in **1** is larger than that in **2**.

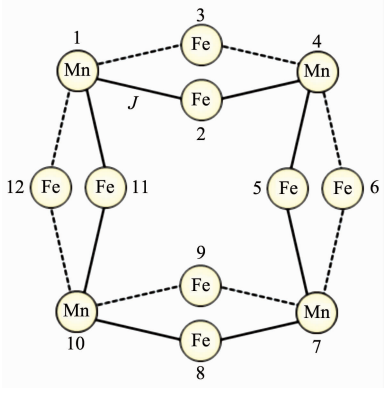

Fig.3　Representation of the magnetic exchange pathways between neighboring metal ions in **1** and **2**

The field dependence of the magnetization (0~50 kOe) measured at 1.8 K is shown in Fig.4. The magnetization increases almost linearly with the applied magnetic field, reaching a value of 3.01$N\beta$ for **1** and 3.38$N\beta$ for **2** at 50 kOe. This behavior is consistent with the antiferromagnetic behavior of **1** and **2**.

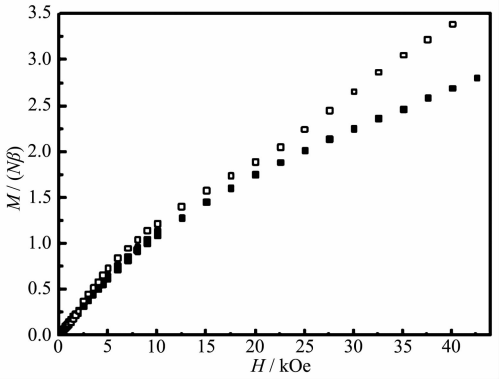

Fig.4　Field dependence of the magnetization at 1.8 K for complexes **1** (■) and **2** (□)

3　Conclusions

In summary, two isostructural cyano-bridged $\{Fe^{Ⅲ}_2Mn^{Ⅱ}\}$ 2D layers were synthesized. The interchain linkage and apical directions of $Mn^{Ⅱ}$ could be fixed via the rigid ditopic ligand bib. The antiferromagnetic interaction between $Fe^{Ⅲ}$ and $Mn^{Ⅱ}$ ions could be tuned by changing the capping ligand of $Fe^{Ⅲ}$ ions with different steric hindrances. Such results provide a strategy to synthesize 1D magnetic systems with tunable intrachain magnetic interactions.

References:

[1] (a)Caneschi A, Gatteschi D, Lalioti N, et al. *Angew. Chem. Int. Ed.*, **2001**,**40**:1760-1763

(b)Miyasaka H, Julve M, Yamashita M, et al. *Inorg. Chem.*, **2009**,**48**:3420-3437

[2] (a)Zhang X M, Wang Y Q, Wang K, et al. *Chem. Commun.*, **2011**,**47**:1815-1817

(b)Miyasaka H, Madanbashi T, Sugimoto K, et al. *Chem. Eur. J.*, **2006**,**12**:7028

(c)Bai Y L, Tao J, Wernsdorfer W, et al. *J. Am. Chem. Soc.*, **2006**,**128**:16428-16429

[3] (a)Coronado E, Mascarós J R G and Gastaldo C M. *J. Am. Chem. Soc.*, **2008**,**130**:14987-14989

(b)Zhang Y Z, Tong M L, Chen X M, et al. *Angew. Chem. Int. Ed.*, **2006**,**45**:6310-6314

(c)Venkatakrishnan T S, Sahoo S, Bréfuel N, et al. *J. Am. Chem. Soc.*, **2010**,**132**:6047-6057

(d)Coulon C, Clérac R, Wernsdorfer W, et al. *Phys. Rev. Lett.*, **2009**,**102**:167204-167207

[4] (a)Lescouzec R, Vaissermann J, Ruiz-Prez C, et al. *Angew. Chem.*, **2003**,**115**:1521-1524; *Angew. Chem. Int. Ed.*, **2003**, **42**:1483-1486

(b)Toma L M, Lescouzec R, Lloret F, et al. *Chem. Commun.*, **2003**,**24**:1850-1851

(c)Wang S, Zuo J L, Gao S, et al. *J. Am. Chem. Soc.*, **2004**, **126**:8900-8901

(d)Toma L M, Lescouzec R, Lloret F, et al. *J. Am. Chem. Soc.*, **2006**,**128**:4842-4853

[5] (a)Ferbinteanu M, Miyasaka H, Wernsdorfer W, et al. *J. Am. Chem. Soc.*, **2005**,**127**:3090-3099

(b)Lescouzec R, Toma M L, Vaissermann J, et al. *Coord. Chem. Rev.*, **2005**,**249**:269-27291

(c)Kou H Z, Ni Z H, Liu C M, et al. *New J. Chem.*, **2009**,**33**: 2296-2299

[6] (a)Rinehart J D, Long J R. *Chem. Sci.*, **2011**,**2**:2078-2085

(b)Sun H L, Wang Z M, Gao S. *Coord. Chem. Rev.*, **2010**, **254**:1081-1101

(c)Aubin S M J, Sun Z, Pardi L, et al. *Inorg. Chem.*, **1999**, **38**:5329-5340

[7] (a)Cucinotta G, Perfetti M, Luzon J, et al. *Angew. Chem. Int. Ed.*, **2012**,**51**:1606-1610

(b)Zuo J L, Bartlett B M, You X Z, et al. *J. Am. Chem. Soc.*, **2006**,**128**:7162-7163

(c)Kostakisa G E, Perlepesb S P, Blatovc V A, et al. *Acc. Chem. Res.*, **2005**,**38**:325-334

(d)Berseth P A, Sokol J J, Shores M P, et al. *J. Am. Chem. Soc.*, **2000**,**122**:9655-9662

[8] Kostakisa G E, Perlepesb S P, Blatovc V A, et al. *Acc. Chem. Res.*, **2005**,**38**:325-334

[9] Berseth P A, Sokol J J, Shores M P, et al. *J. Am. Chem. Soc.*, **2000**,**122**:9655-9622

[10]Wen H R, Zuo J L, et al. *Inorg. Chem.*, **2006**,**45**:582-590

[11](a)Liu T, Dong D P, Kanegawa S, et al. *Angew. Chem. Int. Ed.*, **2012**,**51**:4367-4370

(b)Wang S, Zuo J L, Zhou H C, et al. *Angew. Chem. Int. Ed.*, **2004**,**43**:594-597

(c)Dong D P, Liu T, Zheng H, et al. *Inorg. Chem. Comm.*, **2012**,**24**:153-156

[12]Zhang Y Z, Wang B W, Sato O, et al. *Chem. Commun.*, **2010**,**46**:6959-6961

[13]Song X J, Muddassir M, Chen Y, et al. *Dalton Trans.*, **2013**, **42**:1116-1121

[14]Bogani L, Vindigni A, Sessoli R, et al. *J. Mater. Chem.*, **2008**,**18**:4750-4758

[15](a)Harris T D, Bennett M V, Clérac R, et al. *J. Am. Chem. Soc.*, **2010**,**132**:3980-3988

(b)Bernot K, Bogani L, Caneschi A, et al. *J. Am. Chem. Soc.*, **2006**,**128**:7947-7956

(c)Clérac R, Miyasaka H, Yamashita M, et al. *J. Am. Chem. Soc.*, **2002**,**124**:12837-12844

[16](a)Liu T, Zheng H, Kang S, et al. *Nat. Commun.*, **2013**,**4**: 2826-2833

(b)Liu T, Zhang Y J, Kanegawa S, et al. *Angew. Chem. Int. Ed.*, **2010**,**49**:8645-8648

(c)Liu T, Zhang Y J, Kanegawa S, et al. *J. Am. Chem. Soc.*, **2010**,**132**:8250-8251

[17]Ohkoshi S, Tokoro H, Utsunomiya M, et al. *J. Phys. Chem. B*, **2002**,**106**:2423-2425

[18]Lescouëzec R, Vaissermann J, Lloret F, et al. *Inorg. Chem.*, **2002**,**41**:5943-5945

[19]LI Dong-Feng(李东峰), Clérac R, Parkin S, et al. *Inorg. Chem.*, **2006**,**45**:5251-5253

[20]Vlahakis J Z, Mitu S, Roman G, et al. *Bioorganic & Medicinal Chemistry*, **2011**,**19**:6525-6545

[21]DONG Da-Peng(董大鹏), LIU Tao(刘涛), ZHENG Hui(郑慧), et al. *Scince China B*: *Chem.*(中国科学:化学), **2012**,**55** (6):1018-1021

[22]CHEN Man-Sheng (陈满生), LUO Li(罗莉), SUN Wei-Yin (孙为银), et al. *Chinese J. Inorg. Chem.*(无机化学学报), **2010**,**16**(12):2227-2232